X-932-77-189
PREPRINT

TMX 71408

ORBIT DETERMINATION ACCURACIES USING SATELLITE-TO-SATELLITE TRACKING

(NASA-TM-X-71408) ORBIT DETERMINATION ACCURACIES USING SATELLITE-TO-SATELLITE TRACKING (NASA) 38 p HC A03/MF A01 CSCL 03B

N78-10988

Unclas
G3/90 52037

F.O. VONBUN
P.D. ARGENTIERO
P.E. SCHMID

OCTOBER 1977

GSFC — GODDARD SPACE FLIGHT CENTER — GREENBELT, MARYLAND

X-932-77-189
PREPRINT

ORBIT DETERMINATION ACCURACIES
USING
SATELLITE-TO-SATELLITE TRACKING

F. O. Vonbun
P. D. Argentiero
P. E. Schmid

October 1977

GODDARD SPACE FLIGHT CENTER
Greenbelt, Maryland 20771

ORBIT DETERMINATION ACCURACIES USING SATELLITE-TO-SATELLITE TRACKING

F.O. Vonbun
P.D. Argentiero
P.E. Schmid

ABSTRACT

The possibility of utilizing geostationary spacecraft as orbiting tracking stations was first considered by NASA's Goddard Space Flight Center in the early 1960's. However, satellite-to-satellite tracking did not become a reality until 19 April 1975 when the geostationary Applications Technology Satellite-6 (ATS-6) began to relay Doppler data from the near-Earth geodynamics satellite, GEOS-3. Shortly thereafter ATS-6 radio tracking of the NIMBUS-6 weather satellite was initiated. This paper presents results from these satellite-to-satellite experiments in terms of tracking system performance and orbit determination accuracy. The experience gained during these tests is directly applicable to the NASA geostationary Tracking and Data Relay Satellite System (TDRSS) which has a first launch scheduled for mid 1980.

CONTENTS

LIST OF FIGURES

LIST OF TABLES

ORBIT DETERMINATION ACCURACIES
AND
SATELLITE-TO-SATELLITE TRACKING

1.0 INTRODUCTION

The possibility of using geostationary satellites for communications was discussed in the popular literature as early as 1956 (1). The first detailed proposal for a synchronous tracking satellite system for the purposes of orbit determination was provided by Von Bun in 1967 (2, 3). Since then a number of papers (4, 5, 6, 7, 8, 9,) have considered the use of satellite-to-satellite tracking for orbit determination and for gravity field model refinement. These papers mention that with regard to coverage, a satellite-to-satellite tracking system has a significant advantage over ground based tracking systems. For instance, with a single synchronous relay satellite, a satellite-to-satellite tracking system is capable of observing an earth orbiting satellite during almost half of every orbit. Equivalent coverage of a satellite in a high inclination orbit would be difficult to obtain with a ground based system.

In 1968 during the early planning phases of the geostationary ATS-6 and near-Earth NIMBUS-5 experiments it became clear that this satellite configuration would be ideally suited to evaluate the concept of satellite-to-satellite tracking and to provide valuable experience in processing this new data type. The experiment as defined in October 1968 (10) incorporated both radio time delay (range) and Doppler frequency shift (range rate) measurements. This experiment, entitled the "Tracking and Data Relay Experiment" (T&DRE) was conducted as planned except that NIMBUS-6, which was launched June 12, 1975, rather than NIMBUS-5 carried the T&DRE equipment. In early 1972 plans were completed for a very similar ATS-6/GEOS-3 satellite-to-satellite tracking experiment. The GEOS-3 satellite was launched on April 9, 1975. Another satellite-to-satellite tracking effort involving the ATS-6 was the Goddard Apollo-Soyuz Geodynamics Experiment (11) performed during 1975. However the accent of this experiment was gravity anomaly detection rather than orbit determination. The ATS-6, which was the relay satellite for these experiments, was launched on May 30, 1974 and is still in operation.

The results of these experiments are relevant because NASA intends to use the Tracking and Data Relay Satellite system (TDRSS) (12) for operational orbit determination of NASA satellites. The system will consist of two synchronous relay satellites (one at 41 degrees west and one at 171 degrees west) and a common ground station under construction at White Sands, New Mexico. Operations will begin in November 1980. Hence by the early nineteen eighties satellite-to-satellite tracking data will be routinely processed to obtain orbits.

This paper is a report on the results of the ATS-6/GEOS-3 and the ATS-6/NIMBUS-6 satellite-to-satellite tracking orbit determination experiments. The tracking systems used in these experiments differ from the TDRSS, primarily in the use of one rather than two synchronous relay satellites. However the authors believe and simulations mentioned in this paper indicate that the insights gained from the experiments with regard to proper data reduction techniques and expected results are applicable to the TDRSS.

1.1 EXPERIMENT SPACECRAFT

The key to all satellite-to-satellite experiments to date has been the geostationary ATS-6 spacecraft (13, 14). During the past three years the equatorial ATS-6 has been stationed over both the Pacific in proximity of continental U.S.A. and Africa. Accordingly, ATS-6 ground stations have at various times been operated at Rosman, North Carolina; Mojave, California and Madrid, Spain. The near-Earth satellites tracked via ATS-6 have been GEOS-3 (15), Apollo-Soyuz (16), and NIMBUS-6 (17).

The nominal GEOS-3 orbital parameters are a mean altitude of 843 km, an inclination of 115°, an eccentricity of 0.004, and a period of 101.8 min. The orbit parameters were chosen to minimize resonance of the subsatellite trace with any given Earth feature and to provide orbit traces which cover the Earth in a gridwork pattern.

The Apollo-Soyuz mission included the Geodynamics experiment where Apollo was tracked via ATS-6 for the mission duration (15 July to 24 July 1975). The nominal Apollo orbit at insertion was 150 km by 170 km at an inclination of 51.8°.

Finally, the NIMBUS-6 weather satellite is in a Sun synchronous polar orbit with a mean altitude of 1110 km, an inclination of 100°, and a period of 107.4 min.

2.0 SATELLITE-TO-SATELLITE TRACKING

A satellite radio or laser tracking system makes measurements of such parameters as range, range rate, angles and direction cosines to a spacecraft relative to a given tracking station. In two-way tracking a signal is transmitted from a well surveyed ground station to a spacecraft transponder which frequency translates the signal for re-transmission directly back to the ground station or, as in the case of satellite-to-satellite tracking, to another spacecraft. The two-way tracking system developed for the experiments discussed in this paper measures "range" in terms of the round-trip time delay on a 100 kHz tone and range rate in terms of the Doppler shift on a 2 GHz carrier signal (14, 18).

2.1 GEOMETRY

The tracking geometry is shown in figure 1. The ground station transmits a signal to the near Earth satellite via the synchronous spacecraft. This same signal is "turned around" and transmitted (at a slightly offset frequency) back to the ground site again via the high altitude satellite. For purposes of stability NASA geostationary orbits have been maintained at inclinations which extend from 1.5° to 6°. As a consequence the path indicated as R_1 (figure 1) varies as a function of time as does R_2 (13). Because of the radio propagation times involved and the fact that both spacecraft are in motion relative to the ground site, four distinct paths must be considered when interpreting the Doppler (range-rate) and time delay range/measurements (13, 19).

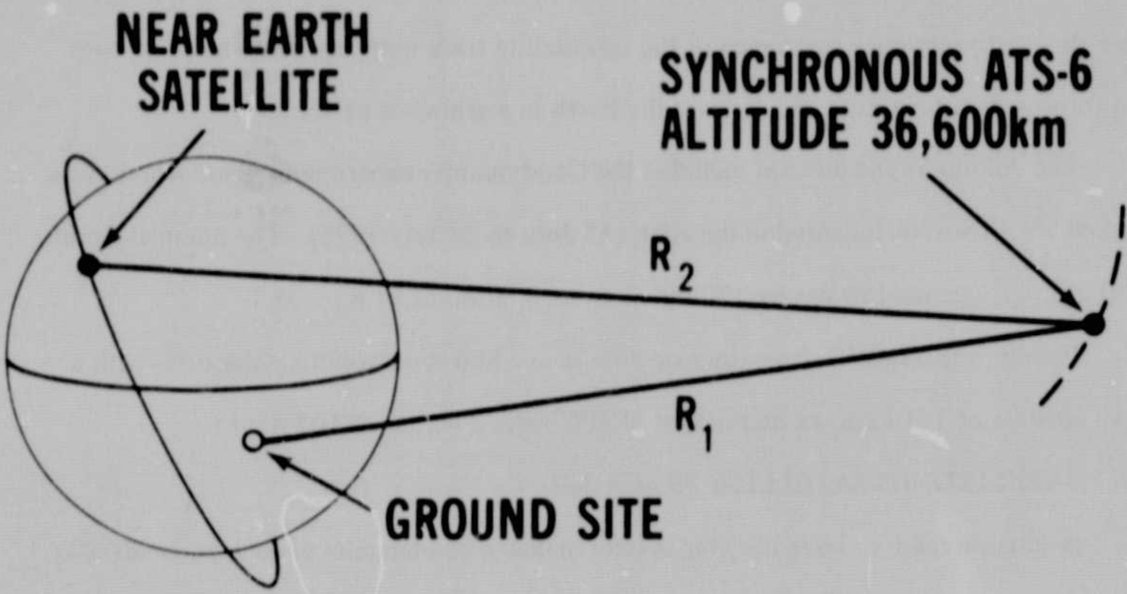

Figure 1. Basic Tracking Geometry

2.2 SYSTEM DESCRIPTION

The "range" measurement is performed by comparing transmitted and received tone zero crossings, the highest resolution tone frequency in this case being 100 KHz. Lower frequency tones are sequentially used during acquisition for ambiguity resolution. The lower tones are at 20 KHz, 4 KHz, 800 Hz, 160 Hz, 32 Hz, and 8 Hz.

The tone ranging measurement is quite straightforward and ranging accuracy depends chiefly on the quality of preflight calibration of both the ATS and NIMBUS transponder group delay. Such preflight calibration data have been taken over a range of frequencies and temperatures. Indications are that with careful calibration the total systematic delay error in the ranging measurement can be held to a few meters of equivalent one-way range.

The "range rate" measurement is performed by counting cycles of Doppler over a measured time interval. In the case of GEOS-3 and Apollo the measurement consisted of the number of Doppler cycles accumulated in the regular sampling interval (1 or 10 seconds depending on mode of operation). For NIMBUS-6 the measurement consisted of the time interval required to accumulate a fixed number of Doppler cycles (18). The electronics for ATS-6 satellite-to-satellite tracking have been so configured that the Doppler output is approximated by:

$$f_d \doteq \frac{-2f_t k}{c} \left[a_1 \bar{\dot{r}}_1 + a_2 (\bar{\dot{r}}_1 + \bar{\dot{r}}_2) \right]$$

where

f_d = measured average Doppler frequency

f_t = uplink frequency

c = speed of light

k, a_1 and a_2 are scalar constants determined by equipment frequency multiplications

$\bar{\dot{r}}_1$ = average range-rate ATS to ground site

$\bar{\dot{r}}_2$ = average range-rate ATS to NIMBUS, Apollo, or GEOS-3

A detailed discussion of Doppler factors in satellite-to-satellite tracking is given in (19). The uplink to ATS-6 (f_t) is at a nominal 6 GHz. The link to and from the low satellite is nominally 2 GHz and ATS-6 back to ground at 4 GHz. The range and Doppler measurements will also be biased by the Earth's troposphere and ionosphere. Measurement biases up to meters in range and tens of cm/sec in range rate can be expected at 2 GHz. Atmosphere refraction effects can to a large extent be modeled out. Some of the work done in this area at NASA-GSFC is indicated in (20, 21, 22). The atmospheric range bias is frequency independent through the troposphere and inversely proportional to frequency squared through the ionosphere. The range rate bias, in addition to the foregoing, is proportional to the rate of scan through the atmosphere as well as to the magnitude of horizontal gradients.

2.3 ORBIT DETERMINATION TECHNIQUES

Problems of Orbit Determination with Satellite-to-Satellite Tracking

The unfamiliar feature of determining user satellite orbits by means of a satellite-to-satellite tracking system is the presence of the relay satellite state as an error source. The simplest procedure for estimating user satellite state in the presence of this error source is to estimate a satellite epoch state from the satellite-to-satellite tracking data with the relay satellite state constrained to a previously determined orbit and left unadjusted in the reduction process. With this approach the uncertainty in relay satellite state is manifested as an unmodeled and time varying error source which alters the estimate of user satellite state. Some subtleties are encountered in determining the effect of this error source. The time history of relay satellite state error is a function of the way in which the epoch state was computed. For example, suppose the relay satellite is independently and continuously tracked over a given period and a least squares algorithm used to estimate epoch state at the beginning of the period. If this epoch state is then propagated to the end of the period using the same dynamic model that was used to process the data, the resultant errors will be constrained by the data fitting criterion implicit in the least squares reduction algorithm. The errors so obtained will be smaller than the errors obtained if either one did not match dynamic models or if one propagated the epoch state beyond the data collection period. The same phenomenon can be understood from a statistical vantage point by observing that when the dynamic models are matched the epoch state errors become correlated with dynamic parameter errors, and that over the data arc these correlations tend to minimize the errors in the epoch state propagation.

Relay satellite state uncertainty appears to be a significant error source even when the relay satellite or satellites are continuously and independently tracked. Argentiero and Loveless (23) simulated the orbit recovery of a satellite in a 300 km, polar, circular orbit with the Tracking Data Relay Satellite System (TDRSS) (24). The TDRSS satellites can relay range and Doppler information from a low altitude user satellite to a ground station. The simulations assumed that each synchronous satellite was continuously tracked from two ground stations and that 24 hour data spans were processed to estimate user satellite state. The same dynamic models which were employed to estimate relay satellite epoch states were also used to estimate user satellite state from the satellite-to-satellite tracking data. The effect of Geopotential and atmospheric drag errors were included in the simulation. The results showed that user satellite position could be recovered with an average total position error of 260 m. The major part of this error is caused by the error in estimates of relay satellite epoch states. When these simulations are repeated without the assumption of continuous tracking the results are considerably worse.

A standard approach to dealing with troublesome error sources in an orbit determination is to augment the list of estimated parameters in the data reduction by including these error sources. This approach can certainly be implemented with regard to relay satellite state errors by simultaneously estimating user and relay satellite epoch states from information supplied by the satellite-to-satellite tracking data. From one vantage point this is an undesirable solution in that the user is uninterested in the state of the relay satellite and would rather not burden the numerical procedures with the need for simultaneously estimating relay satellite state with the user satellite state. However, the results of independent covariance analyses performed by Fang and Gibbs (25), and Argentiero and Garza-Robles (26) indicate that an unconstrained simultaneous estimate of user and relay satellite states using satellite-to-satellite tracking data can yield an estimate of user satellite state which is consistently better than 100 m.

Numerous simultaneous unconstrained solutions have been attempted using range sum and range sum rate measurements obtained from the ATS-6/GEOS-3 combination and the ATS-6/NIMBUS-6 combination and in all cases the solutions have been inaccurate and numerically unstable. Clearly our experience with real reductions of satellite-to-satellite tracking data is not compatible with the results of previous error studies. In order to understand the discrepancy we have performed a numerical simulation of the ATS-6/GEOS-3 satellite-to-satellite tracking experiment. The difference between a numerical simulation and a covariance analysis can be described as follows: in a simulation, data are generated and a least squares adjustment process is actually performed. The estimated state is then compared to the reference or unperturbed state at various points along the orbit and conclusions can be drawn concerning the accuracy of the process. In a covariance analysis mode, the least squares adjustment process is postulated rather than actually performed, and under the assumption that over the range of expected errors, perturbations of orbital estimates are approximately linear functions of perturbations of the error sources, the associated covariance matrix of the epoch state recovery is computed. With the aid of state transition matrices the covariance matrix at epoch can be propagated to obtain the covariance matrix of the satellite state recovery at any point in the orbit.

For the numerical simulation a computer program was used to generate 12 hours of range and Doppler satellite-to-satellite tracking data from the ATS-6/GEOS-3 satellite combination. In this data generation the Naval Weapons Laboratory (NWL) geopotential field was used. A random number generator added white noise of standard deviation 1 mm/sec to the Doppler data and white noise of 2 m to the ranging data, values consistent with tracking system performance. The SAO 69 geopotential field and an orbit determination program were used to reduce the data to simultaneously estimate the ATS-6 and GEOS-3 epoch states. The estimates GEOS-3 epoch state was propagated along the entire 12 hour data collection period using the SAO 69 geopotential field. This orbit was compared at selected time points to the true GEOS-3 orbit which was obtained by propagating the GEOS-3 reference epoch state with the NWL geopotential field. The average difference between the two orbits was over 900 m. Also the nominal covariance matrix of the data reduction revealed that several correlations between estimated parameters were of absolute value near unity. This implies that the normal matrix which is inverted in the least squares estimation process is poorly conditioned. Hence small perturbations of the elements of this matrix such as those caused by computer roundoff and other effects cause major perturbations of the elements in the inverted matrix. This amplification effect in the inversion of a poorly conditioned matrix can lead to an inaccurate estimate of a satellite epoch state or in some cases a divergence of the least squares interation procedure. This is the probable cause of poor results using a simultaneous estimation approach in both the simulated and real data reductions. In a covariance analysis of the simultaneous estimation approach the least squares algorithm is not actually executed and consequently these numerical problems are never manifested. For this reason the techniques of covariance analysis provide a somewhat optimistic assessment of orbital accuracies obtainable from simultaneous estimation with satellite-to-satellite tracking data.

Thus the two conclusions of our analyses are: 1) The uncertainty in relay satellite state is a significant error source which cannot be ignored in the reduction of satellite-to-satellite tracking data and 2) that based on both simulations and real data reductions it is numerically impractical to use simultaneous unconstrained solutions to determine both relay satellite and and user satellite epoch states. The estimation technique used to generate the results shown in subsequent sections may be described as a Bayesian or least squares with a-priori procedure. This approach permits the adjustment of relay satellite epoch state in the reduction of satellite-to-satellite tracking data but without the numerical difficulties introduced by an ill-conditioned normal matrix. Theoretically this technique obtains the best possible estimate of user satellite state based on all available information. A mathematical description follows.

Mathematical Description

In this mathematical development we assume the existence of two separate data sets:

y_1 – Ranging observations between ATS-6 and ground based tracking stations

y_2 – Satellite-to-satellite tracking of user satellite (range sum and range rate sum) with ATS-6 as relay satellite.

The parameter set to be estimated consists of two satellite epoch states.

x_1 – Six dimensional ATS-6 state at epoch time T_1

x_2 – Six dimensional user satellite state at epoch time T_2

The data set y_1 is corrupted by errors in the measuring process. Hence represent y_1 as:

$$y_1 = \tilde{y}_1 + v_1,\ e(v_1) = \overline{0},\ e(v_1 v_1^T) = Q_1 \tag{1}$$

where $\tilde{y}_1$ is the correct or noiseless representation of the data set, v_1 is a vector of random errors of zero expectation and covariance matrix Q_1. Describe the functional relationship between $\tilde{y}_1$ and x_1 as

$$\tilde{y}_1 = f(x_1) \tag{2}$$

The right side of eq. 2 represents a computational algorithm obtained by integrating satellite motion to each observation time and computing the ideal observations. The standard least squares estimator $\hat{x}_1$ of x_1 is that vector which minimizes the loss function.

$$L(\hat{x}_1) = (y_1 - f(\hat{x}_1))^T Q_1^{-1} (y_1 - f(\hat{x}_1)) \tag{3}$$

Assuming the linearity of eq. 2, the vector which minimizes the right side of eq. 3 is also known to be a minimum variance estimator. A first approximation to the desired minimum can be obtained by expanding equation 2 in a first order Taylor series about nominal value $x_{1,n}$

$$\delta\tilde{y}_1 = A_1 \delta x_1,\ A_1 = \left.\frac{\partial f(x_1)}{\partial x_1}\right|_{x_1 = x_{1,n}} \tag{4}$$

where $\delta\tilde{y}_1$ and δx_1 are deviations of $\tilde{y}_1$ and x_1 from nominal values and A_1 is the so-called sensitivity matrix. The estimate of δx_1 is

$$\delta\hat{x}_1 = (A_1{}^T Q_1{}^{-1} A_1)^{-1} A_1{}^T Q_1{}^{-1} \delta y_1 \tag{5}$$

where

$$\delta y_1 = y_1 - f(x_{1,n})$$

The vector $\delta\hat{x}_1$ is added to $x_{1,n}$ to form an estimate of $\hat{x}_1$. This estimate can be used as a new nominal and the process can be repeated until a convergence criterion is satisfied. The covariance matrix of the least squares estimate $\hat{x}_1$ of x_1 is

$$c = e([\hat{x}_1 - x_1]\ [\hat{x}_1 - x_1]^T) = (A^T Q_1{}^{-1} A)^{-1} \tag{6}$$

The next step is to obtain an optimal processing of the data set y_2. Define a 12 dimensional vector z as

$$z = \begin{bmatrix} x_2 \\ x_1 \end{bmatrix} \tag{7}$$

Represent the data set y_2 as

$$y_2 = \tilde{y}_2 + v_2,\ e(v_2) = \overline{0},\ e(v_2 v_2{}^T) = Q_2 \tag{8}$$

where $\tilde{y}_2$ is the correct or noiseless representation of the data set, v_2 is a vector of random errors of zero expectation and covariance matrix Q_2. The functional representation between $\tilde{y}_2$ and z is presented as.

$$\tilde{y}_2 = g(z) \tag{9}$$

As was the case with equation 2, the right side of eq. 9 represents a computational algorithm involving the integration of satellite equations of motion.

The least squares estimate of z would not be optimal unless all available information were included in the loss function. Hence it is appropriate to treat the least squares or minimum variance estimate $\hat{x}_1$ of x_1 as an a-priori estimate weighted by the inverse of the covariance matrix provided by equation 6. The resulting loss function to be minimized is

$$L(z) = (y_2 - g(z))^T Q_2^{-1} (y_2 - g(z)) + \left(z - \begin{bmatrix} \bar{o} \\ \hat{x}_1 \end{bmatrix}\right)^T \begin{pmatrix} \bar{o} & \bar{o} \\ o & c^{-1} \end{pmatrix} \left(z - \begin{bmatrix} \bar{o} \\ \hat{x}_1 \end{bmatrix}\right) \tag{10}$$

Again, the required minimum can be obtained iteratively by expanding equation eq. 9 in a first order Taylor series about a nominal estimate z_n of Z

$$\delta\tilde{y}_2 = A_2 \delta z, \; A_2 = \left.\frac{\partial g(z)}{\partial z}\right|_{z=z_n} \tag{11}$$

where $\delta\tilde{y}_2$ and δz are deviations of $\tilde{y}_2$ and z from nominal values and A_2 is the sensitivity matrix. The estimate of δz is

$$\delta\hat{z} = \left(A_2^T Q_2^{-1} A_2 + c^{-1}\right)^{-1} \left(A_2^T Q_2^{-1} \delta y_2 + \begin{bmatrix} \bar{o} & \bar{o} \\ \bar{o} & c^{-1} \end{bmatrix} \begin{bmatrix} \bar{o} \\ \delta\hat{x}_1 \end{bmatrix}\right) \tag{12}$$

where

$$\delta\hat{x}_1 = \hat{x}_1 - x_{1,n}, \; \delta y_2 = y_2 - g(z_n)$$

The vector $\delta\hat{z}$ is added to z_n to estimate $\hat{z}$. This estimate is used as a new nominal and the process is repeated until a convergence criterion is satisfied. The final covariance matrix for the estimate of satellite state x_1 and satellite state x_2 is

$$E\left[\left(\hat{z} - \begin{bmatrix} x_1 \\ x_2 \end{bmatrix}\right)\left(\hat{z} - \begin{bmatrix} x_1 \\ x_2 \end{bmatrix}\right)^T\right] = \left(A_2^T Q_2^{-1} A_2 + c^{-1}\right)^{-1} \tag{13}$$

It can be shown that the two step process defined above in which data set y_1 is processed and then data set y_2 is processed is equivalent to a single step unconstrained least squares estimation of x_1 and x_2 using both data sets y_1 and y_2. Hence this procedure leads to the most accurate estimate of both user and relay satellite state based on available information.

3.0 EXPERIMENTAL RESULTS

The experimental results can be considered in three categories – namely,

- tracking system performance
- geostationary satellite orbit evaluation
- near Earth satellite orbit evaluation

3.1 TRACKING SYSTEM PERFORMANCE

The expected error for the NASA range and range rate satellite-to-satellite tracking system is a function of many controlled parameters such as range tone frequency, sample rate, bandwidth settings, signal-to-noise spectral density ratios, spacecraft dynamics, etc, (13). However, the system is generally used with what might be termed a standard set of options such as: 100 kHz maximum range tone frequency, signal levels such that system is not thermal noise limited, 1 per second or 6 per minute data rate, and a 25 Hz range tracking loop two-sided noise bandwidth. Table I lists the theoretical system performance for the foregoing selected options. Doppler averaging time is approximately one half the sample time interval for NIMBUS tracking and equal to the sample interval for Apollo and GEOS tracking.

For averaging times, T, up to about 10 seconds the noise decreases as 1/T. The principal Doppler noise contribution comes from receiver voltage controlled crystal oscillators and the analog to digital conversion. For longer integration times the Doppler noise is also influenced by noise falling off as 1/T, an effect attributed to the phase jitter in the

TABLE I

Tracking System Measurement Resolution

Range (Meters)		Range Rate (Cm/Sec)	
Systematic	Random	Systematic	Random
1.2	1.2	Negligible	0.03
		NOTE: 10 Sec. Averaging	

transmitter reference signal used at the Doppler extractor. For satellite-to-satellite tracking involving ATS-6 the range-rate resolution for T seconds of averaging (27) is given by:

$$\sigma_{\dot{R}} = \sqrt{\left(\frac{0.3}{T}\right)^2 + \left(\frac{0.07}{\sqrt{T}}\right)^2} \text{ cm/sec}$$

This range-rate resolution versus Doppler measurement averaging time is plotted in Figure 2.

It should be mentioned that the least significant range bit recorded is 1.5 meters which is consistent with the best expected one way performance of 1.7 meters resolution. Measured results indicate close agreement with expected system performance. System random errors or "noise" are generally observed by the least squares fitting of short data spans (i.e., 1 to 10 minutes) with polynomials of at least 5th degree to account for spacecraft dynamics. Care must be taken such that the polynomial itself does not introduce apparent error. If the data is from a static or collimation tower test a least squares straight line fit is appropriate.

Assuming reasonable tracking geometry the accuracy of spacecraft position and velocity determination will be primarily limited by tracking system performance for any computation spanning the data collection interval. That is, if continuous tracking is provided from a set of well surveyed stations the computation is essentially one of geometry. On the other hand the accuracy of orbit prediction based on an initial spacecraft vector

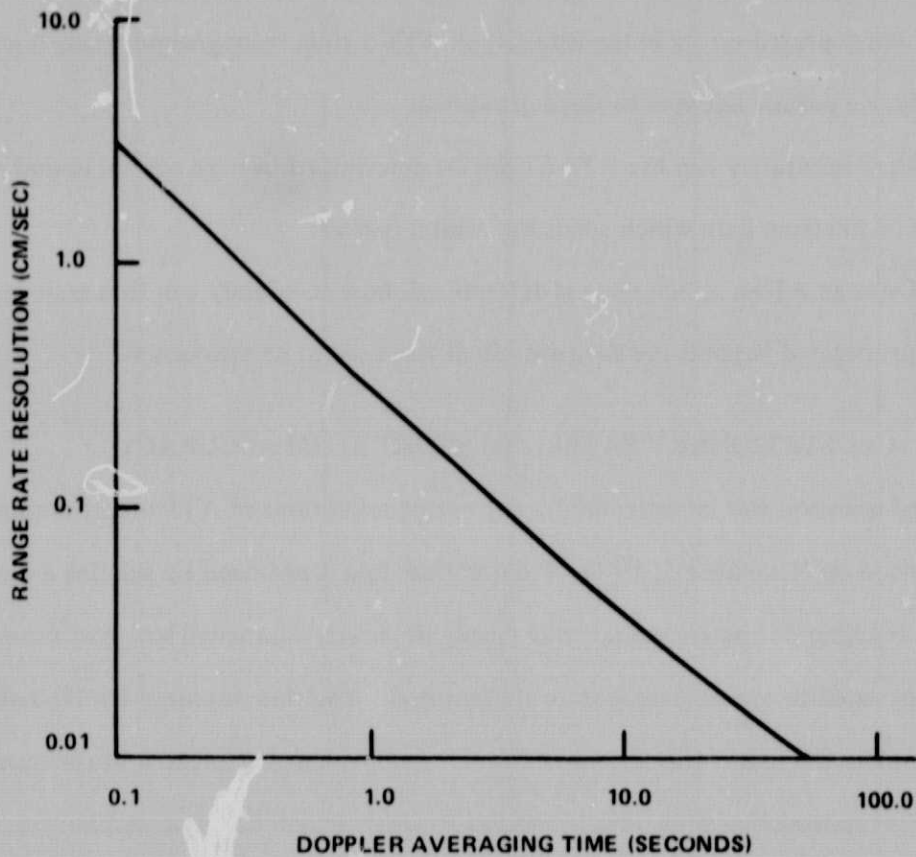

Figure 2. Range Rate Resolution

determination will be degraded as a function of time in direct relation to the accuracy to which physical parameters are modeled. This modeling includes gravitational fields, atmospheric drag and refraction effects, solar pressure, station location determination and so on. The most critical of these modeling parameters in terms of orbit determination accuracy is the gravity field model which at present is generally expressed in terms of a spherical harmonic expansion.

3.2 ATS-6 ORBIT DETERMINATION RESULTS

The optimal reduction of satellite-to-satellite tracking data to determine a user satellite orbit requires an accurate a priori estimate of relay satellite state. Hence, it is important to determine the expected errors in the estimate of ATS-6 state from ground based tracking. More precisely, we require answers to these questions:

1) How accurately can the ATS-6 orbit be determined over an orbital period (24 hr) from data which spans the orbital period?

2) Once an ATS-6 epoch state is determined, how accurately can that state be propagated beyond the data arc which was used in its estimation?

GEOSTATIONARY SATELLITE SHORT TERM ACCURACY

The first question was investigated by examining reductions of ATS-6 trilateration tracking obtained on November 3, 1974. Trilateration data is obtained by sending a signal from a single tracking station to several strategically deployed unmanned low cost transponders via the satellite whose state is to be determined. The time required for the radio signals to complete the round trip to and from each transponder is measured at the transmitter site. The interrogating sites were located at Rosman, North Carolina and Mojave, California. The transponders were located at Rosman, Mojave, Greenbelt, Maryland, and Santiago, Chile.

The method of "orbit overlaps" was used to evaluate the orbit determination accuracy of the system. This procedure can be outlined as follows:

1) Determine a satellite epoch state using each of two independent data sets

2) Propagate estimated epoch states over a common or overlapping interval

3) Difference the two orbits over the common interval (differences are usually displayed in along track, cross track, and radial components).

In some cases the orbit overlap method can lead to an under-estimation of orbit errors since biases in orbit estimates may cancel in orbit differences. Hence, the method should be viewed as a test of the internal consistency of an orbit determination process rather than an absolute measure of accuracy. Data set 1 used in the orbit overlap test was obtained with Rosman as a transmitting site and with transponders at Rosman, Mojave, Greenbelt, and Santiago. Data set 2 was obtained with the same transponder sites but with the transmitter located at Mojave. The tracking schedule is shown in figure 3. The two interrogating sites are identified in figure 3 under TRANSMITTER as Rosman, North Carolina and the Mojave, California "Hybrid Transportable" station. Each data stretch was approximately 5 minutes long and the data rate was one sample per 10 seconds. Separate orbit arcs were computed from data set 1 and data set 2. The total position differences between the two orbits over the 24 hours of Nov. 3, 1974 were computed and are displayed in figure 4. The mean position error is about 100 m. A typical set of range residuals is shown in figure 5. The range residuals over this arc are on the order of 20 m.

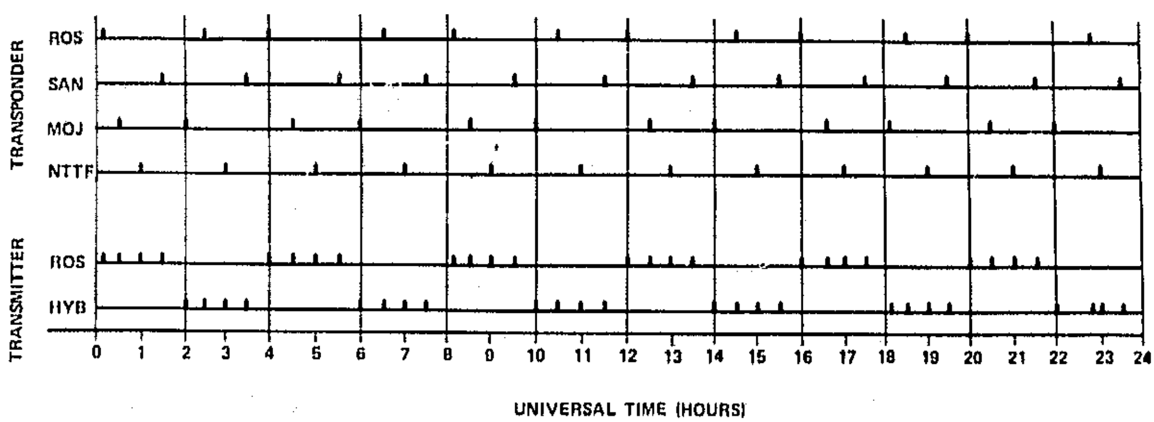

Figure 3. Tracking Schedule 3 November 1974

Assuming that there are no significant biases in the trilateration orbit determination whose effects cancel in the orbit overlap test, the results of figure 4 suggest that continuous tracking of ATS-6 over a 24 hour period leads to an orbit estimate over the period which is accurate to about 100 m.

ORIGINAL PAGE IS
OF POOR QUALITY

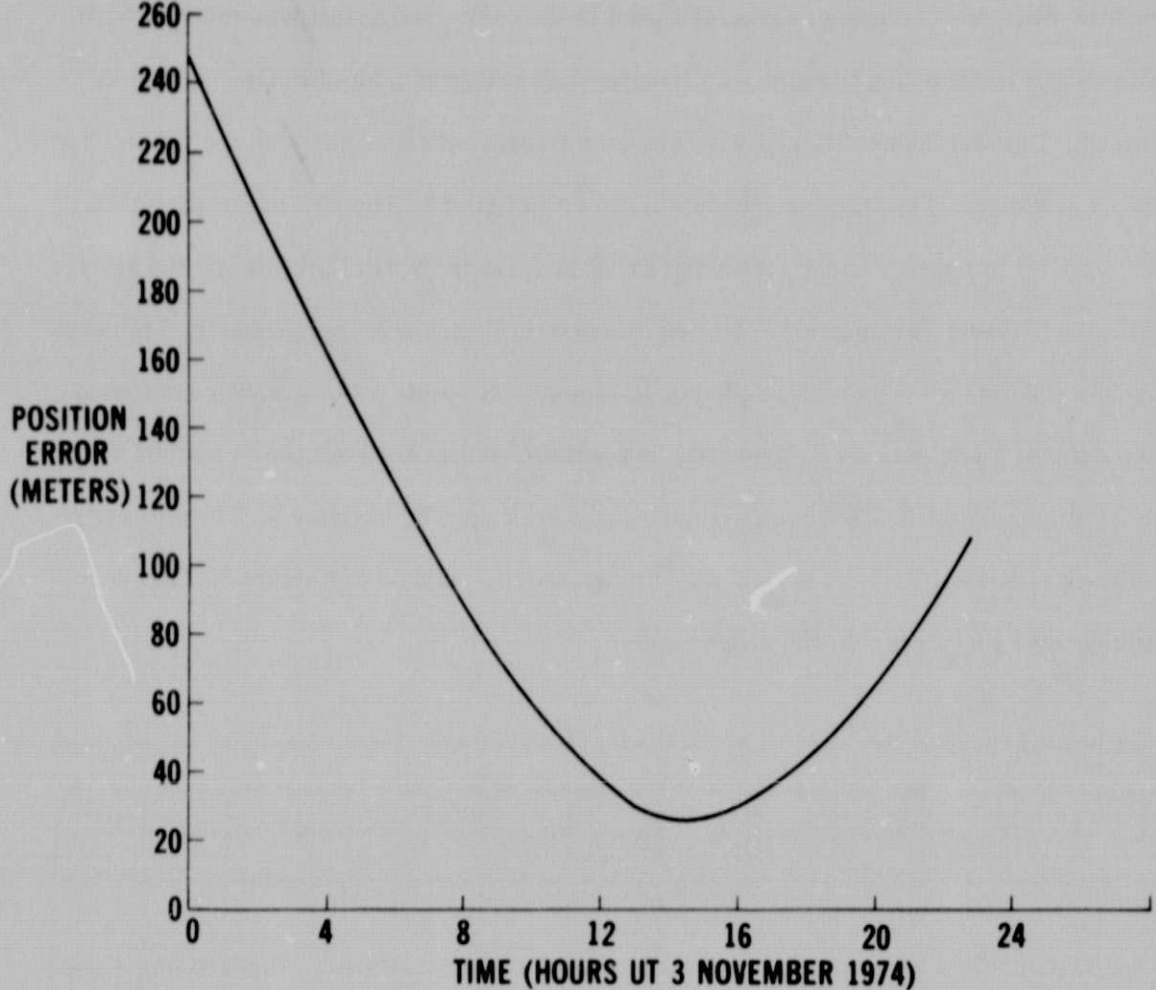

Figure 4. ATS-6 Total Position Error

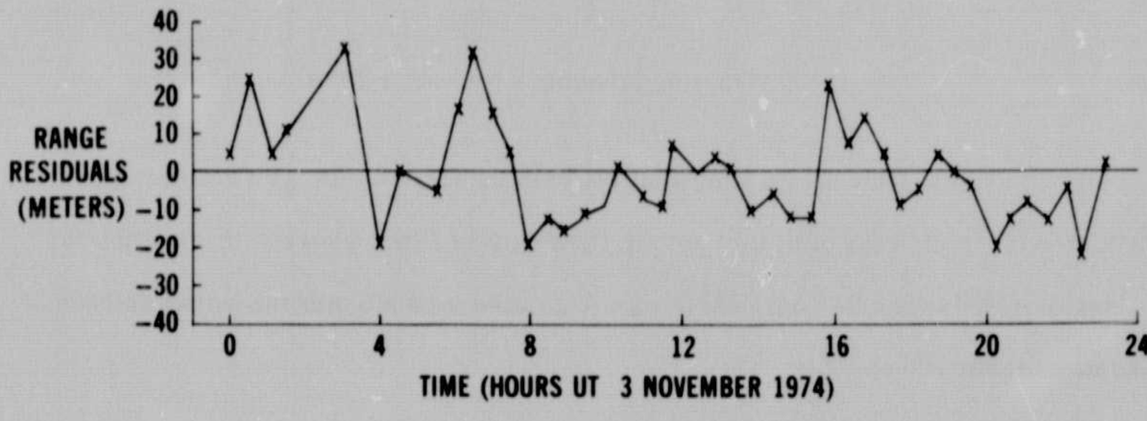

Figure 5. ATS-6 Orbit Residuals

GEOSTATIONARY SATELLITE LONG-TERM ACCURACY

In general one cannot assume that relay satellites are continuously tracked. Hence, in the reduction of satellite-to-satellite tracking data, it may be necessary to use an estimate of user satellite state obtained through a propagation that was unconstrained by the data fitting criterion of a least squares algorithm. When this occurs the accuracy of the orbit estimate is entirely dependent on the correctness of the force models used in the propagation.

The orbit overlap technique (30), utilizing data obtained during July 1975 was used to estimate the accuracy of a free or unconstrained propagation of an ATS-6 epoch state. The data sets used in the overlap tests were:

Data Set 1 – 24 hours of data over July 13, 14, 1975. Tracking stations located at Madrid, Ascension Island, and Johannesburg.

Data Set 2 – 24 hours of ranging data over July 25, 1975. Tracking stations located at Madrid, Ascension Island, and Johannesburg.

Each data set was processed to estimate an ATS-6 state vector for epoch time July 16, 1975 at 7 hr., 25 min. The epoch states were propagated forward for 10 days and along track, cross track, and radial differences were computed at 15 minute intervals. The root mean square along track difference was over 2 km. Figure 6 is a plot of these along track differences.

The large errors which occur during the free propagation of an ATS-6 epoch vector must be caused by a misrepresentation of force models. The obvious candidates are:

1) Unmodeled venting and thrusting of ATS-6 to accomplish satellite attitude corrections. Motions due to antenna maneuvering may also introduce errors.

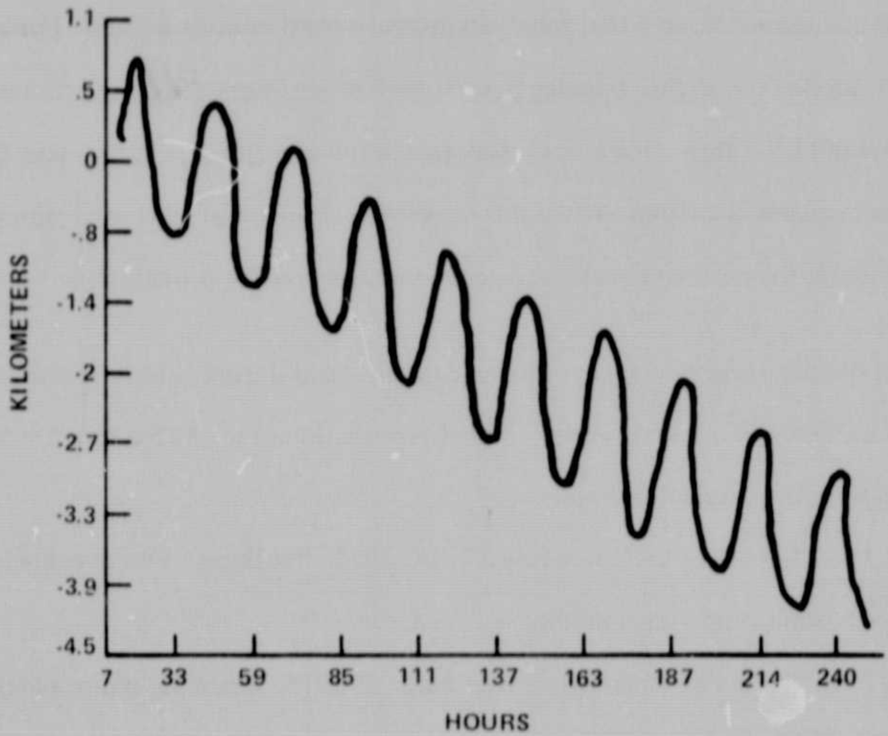

Figure 6. Along Track Orbit Differences for ATS-6 Overlap Test, July, 1975

2) Mismodeling of solar radiation pressure. In all data reductions, ATS-6 was assumed to present a constant cross section to the sun. In fact, this is not the case.

3) An error in representation of the central force term of the Earth's gravity field. An estimate of the uncertainty in estimates of this parameter is one part in 10^6.

Error source number 3 appeared to us as the most likely cause for the major part of the errors exhibited in figure 6. In order to measure the effect of uncertainty in the gravity field parameter on the free propagation of ATS-6, the following simulation was performed; ranging observations to the ATS-6 from sites at Rosman, Santiago, and Mojave were generated for a three day span. The observations were corrupted with white noise with a standard deviation of 10 m. The value of the gravity field parameter used to generate the data was perturbed by one part in 10^6 and this value was used along with a least squares estimator to estimate an epoch state at the beginning of the three day data span. The perturbed value of the gravity field parameter was used to propagate this epoch state for six days. Over the three days covered by data the propagated orbit differed from the assumed true orbit by about 100 m. But at the end of the six day propagation period the errors were approximately 2 km. The results of this simulation suggest that the error in the central force term of the Earth's gravity field is sufficient to account for the errors in the ATS-6 free propagation as manifested in figure 6.

SUMMARY OF RESULTS

Overlap tests performed with real data together with simulation results suggest that by processing data over one ATS-6 orbital period, the ATS-6 state over the orbital period can be determined with an average accuracy of about 100 m. But other results show that when longer data arcs are used or when an estimated ATS-6 epoch state is propagated well beyond the data arc used in its estimation, errors in the kilometer region are encountered. These facts indicate that there are significant errors in the models of the forces acting on the ATS-6. The most likely candidate is the error in representation of the central force term of the gravity field.

3.3 GEOS-3 ORBIT DETERMINATION RESULTS

The GEOS-3 orbit determination results were derived from data obtained over the weekend of May 3, 1975. The tracking schedules and the tracking systems used in the evaluation are shown in figure 7. The figure shows that five passes of range sum and range sum rate data were available. A Bayesian estimation technique described in a previous section was used to obtain two separate and overlapping GEOS-3 orbits. A GEOS-3 epoch state at May 2, 22 hr was estimated using all the ATS-6 ranging data and the first three passes of

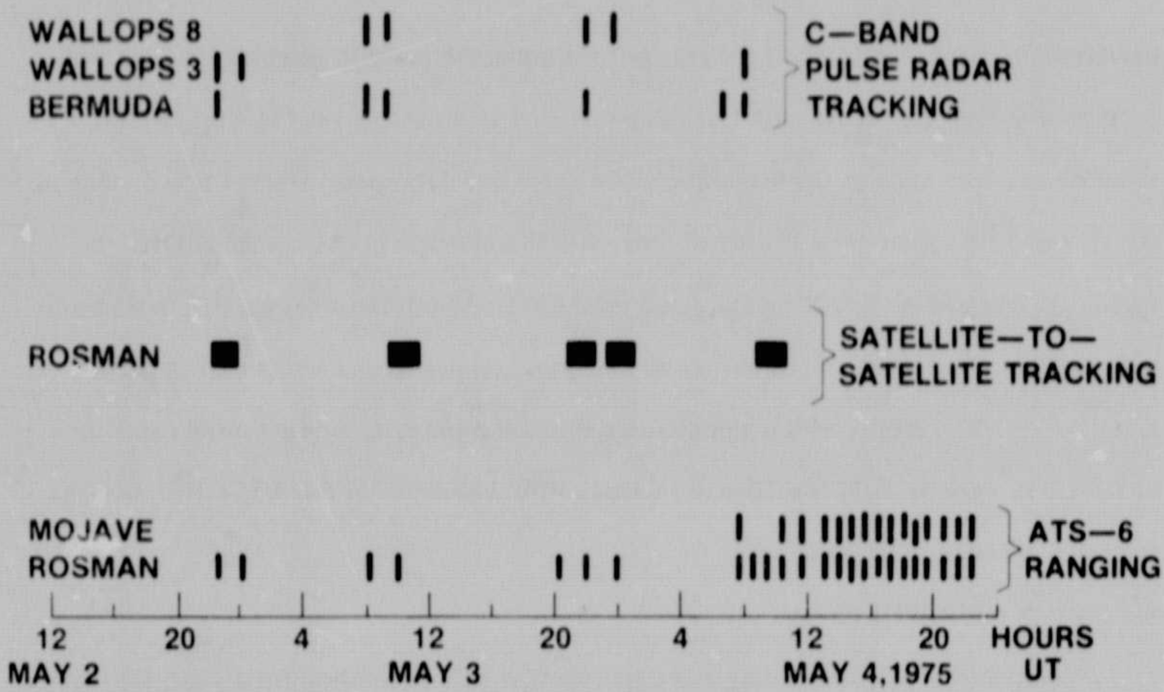

Figure 7. Data Summary

range sum and range sum rate data. The ATS-6 ranging data was weighted according to a standard deviation of 2 m. The range sum and range sum rate data were weighted according to standard deviations respectively of 2 m and 1 mm/sec. The complete GEM-7 geopotential field was used in this and all other data reductions. The estimated epoch state was propagated to the end of the data span of May 3, 22 hr. The process was repeated with the last four passes of range sum and range sum rate data to estimate a GEOS-3 epoch state at May 3, 10 hr. This epoch state was propagated to the end of its data span at May 4, 10 hr. The total position difference between the two orbits during the 12 hr overlap period as shown in figure 8 varies periodically between 10 and 25 meters.

As mentioned in a previous section, orbit overlap procedures can provide an overly optimistic assessment of orbit determination accuracy. A more objective measure of accuracy is obtained by comparison with an orbit derived from an independent and well calibrated data set. Figure 7 displays the C-band tracking available from Wallops Island and Bermuda during the weekend of May 3, 1975. A three-day GEOS-3 arc was derived from the C-band data and compared to a similar arc derived from the five passes of satellite-to-satellite tracking data and ATS-6 ranging data. The root mean square differences in the two arcs were:

radial	5 m
cross track	200 m
along track	39 m

Various orbit results indicate that total position error for C-band derived GEOS-C orbits is on the order of 50 m (31). Hence, it is only in the cross track direction that the orbit determination derived from satellite-to-satellite tracking data differs significantly from the C-band orbit. The large cross track errors can be explained in terms of the tracking geometry. For each of the five satellite-to-satellite tracking passes shown on figure 7, the GEOS-3 satellite passed almost directly under the ATS-6 satellite. Consequently there was little cross track information in the range sum and range sum rate data. It is a reasonable assumption that with a better geometric distribution of passes the cross track errors would be substantially reduced.

3.4 NIMBUS-6 ORBIT DETERMINATION RESULTS

The NIMBUS-6 overlap results were derived from data obtained over the weekend of Feb 8, 1976. For this experiment a highly accurate reference orbit suitable for the purpose of comparison was unavailable. This implied that the primary measure of the quality of the orbits derived from satellite-to-satellite tracking would be obtained from orbit overlap test. Hence the orbit overlap test for the ATS-6/NIMBUS-6 experiment was performed in a way which was more rigorous and less optimistic than the overlap test performed for the ATS-6/GEOS-3 experiment. Notice that for the ATS-6/GEOS-3 experiment the overlap test was performed with data sets which intersected through the entire overlap interval. Hence both orbits used in the comparison were constrained by data at each end of the interval. With such a procedure it is possible for the effects of errors in the measuring system to cancel in the test results. It will be seen that for the ATS-6/NIMBUS-6 overlap test the two data sets in question are abuting rather than overlaping and effect of measurement system errors are less likely to cancel in the test results.

The tracking schedules and the tracking systems used in the evaluation are shown in figure 9. The first two rows of this figure show the tracking schedules for the ranging data from Madrid, Spain to ATS-6, and from Ahmedabad, India to ATS-6. The third row

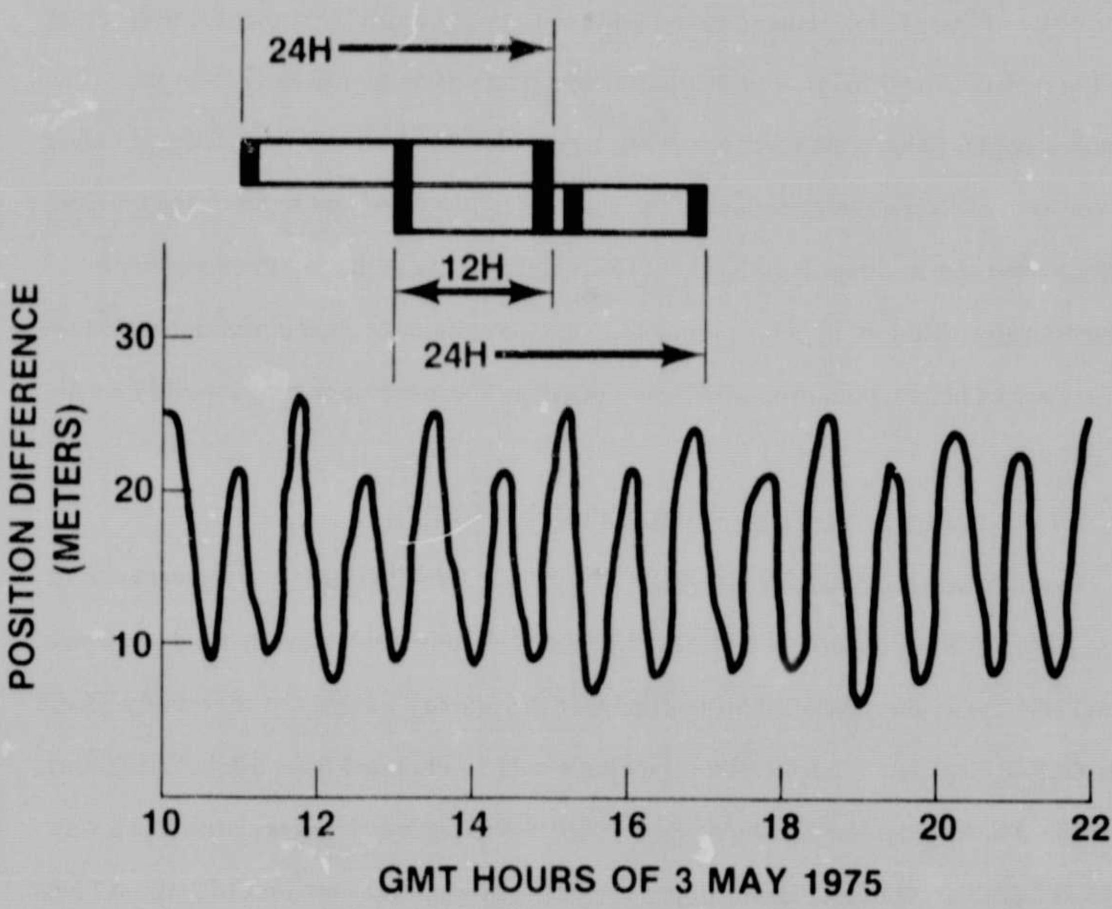

Figure 8. GEOS-3 Overlap Position Differences

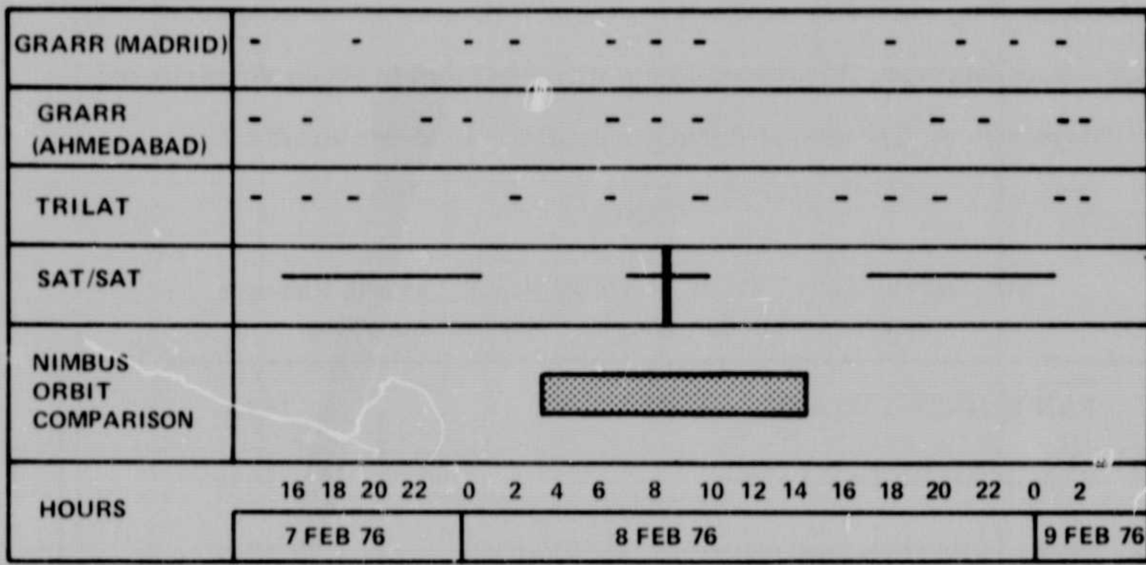

NOTE: DATA ON LEFT HAND SIDE OF VERTICAL BAR IN SAT/SAT ROW USED FOR RECOVERY OF FIRST NIMBUS EPOCH VECTOR, DATA ON RIGHT HAND SIDE USED FOR RECOVERY OF SECOND NIMBUS EPOCH VECTOR.

Figure 9. Measurement Periods and Period for Nimbus Orbit Comparison

indicates the tracking schedule for trilateration data (Madrid-ATS-6-Ascension Island). The fourth row shows the tracking schedule for the range sum and range sum rate data with Madrid as the ground station. The vertical bar located at 9HR/UT Feb. 8 indicates the epoch time for two estimated NIMBUS-6 epoch states. Epoch state 1 was obtained by executing a Bayesian least squares estimator with all the ATS-6 ranging and trilateration data and all the satellite-to-satellite tracking data to the left of the epoch time. Epoch state 2 was obtained by repeating the procedure with the satellite-to-satellite tracking data to the right of the epoch time replacing the data to the left of the epoch time. The horizontal bar in row 5 of the figure displays the common interval over which the two NIMBUS-6 epoch states were propagated. The complete GEM-7 gravity field model was used in all data reductions and propagations. The relative weights for the data types were obtained by first using nominal weights and processing all the data to estimate ATS-6 and NIMBUS-6 epoch states.

The residuals of the estimation were used to determine the standard deviations of the noise on the various data types. These standard deviations were used to obtain weights for the final data reductions. The computed standard deviations are shown on table 2.

TABLE 2

Standard Deviation Used for Weighting Measurements in Nimbus-6 Satellite-to-Satellite Tracking Orbit Determination

RANGE (INDIA) TO ATS	168 m
RANGE (MADRID) TO ATS	50 m
TRILATERATION (MADRID, ATS, ASCENSION)	15 m
SATELLITE-TO-SATELLITE RANGE	11 m
SATELLITE-TO-SATELLITE RANGE RATE	.3 cm/sec

The data reductions were complicated by the fact that an experiment onboard the NIMBUS-6 was responsible for some outgasing. This effect was modeled as a constant along track thrust whose magnitude was estimated in the data reductions. The recovered magnitude was approximately 10^{-7} m/sec^2.

Figures 10, 11, and 12 display the along track, cross track, and radial differences in the two epoch state propagations during the overlaping period. The R.M.S. differences are 40 m along track, 30 m cross track, and 12 m radial. The secular growth of residuals in the along track direction is explainable in terms of gravity field error and an imperfect modeling of the outgasing effect whose direction was probably not exactly along track and whose magnitude was probably not constant.

Finally it should be mentioned that a NIMBUS-6 orbit derived from satellite-to-satellite tracking data was compared to a NIMBUS-6 orbit derived from minitrack data. The orbit differences were well within the stated accuracy for minitrack orbits of 500 m.

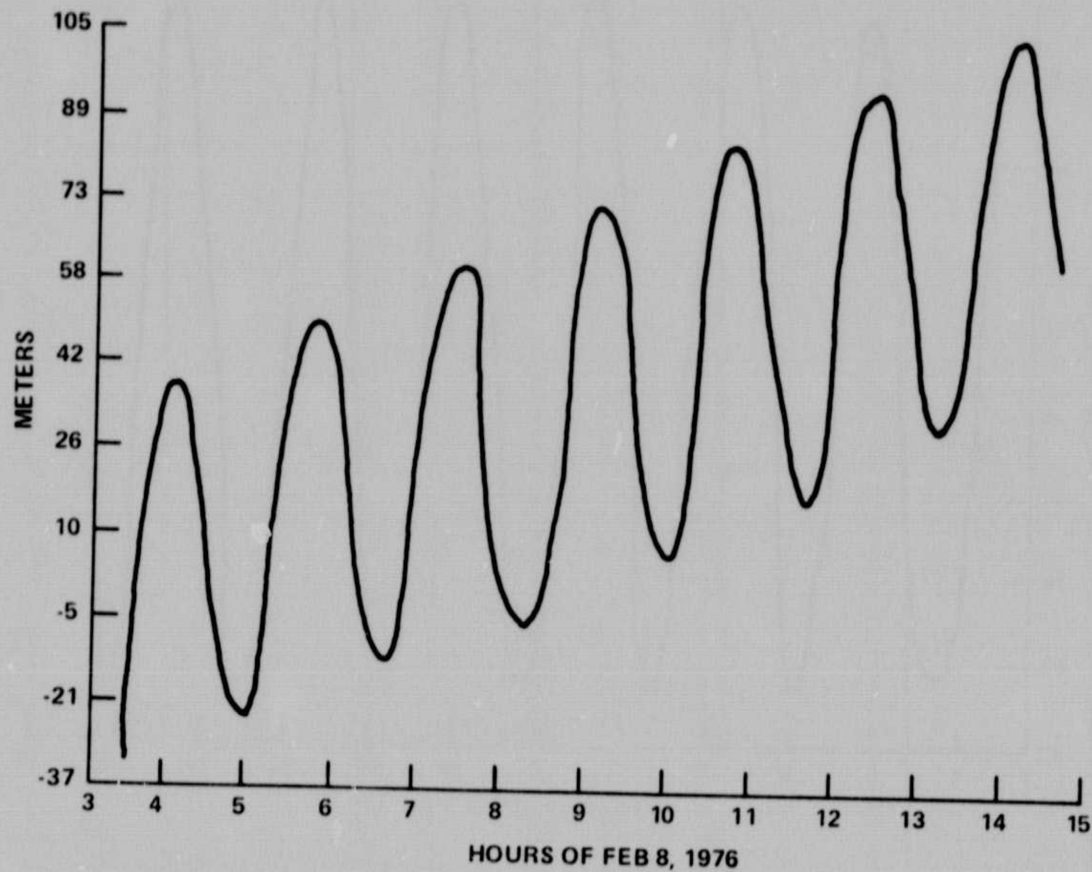

Figure 10. Along Track Differences for Nimbus-6 Satellite-to-Satellite Tracking Orbit Determination

4.0 CONCLUSIONS

The ATS-6/NIMBUS-6 and ATS-6/GEOS-3 satellite-to-satellite radio tracking system performs as specified with a resolution of 1 meter in range and .03 cm/sec in range-rate for a 10 second averaging.

A Bayesian least squares estimation technique utilizing a good a priori estimate of relay satellite state was used during these experiments to obtain user satellite orbits with accuracies comparable to what is obtainable from ground tracking systems. The limiting

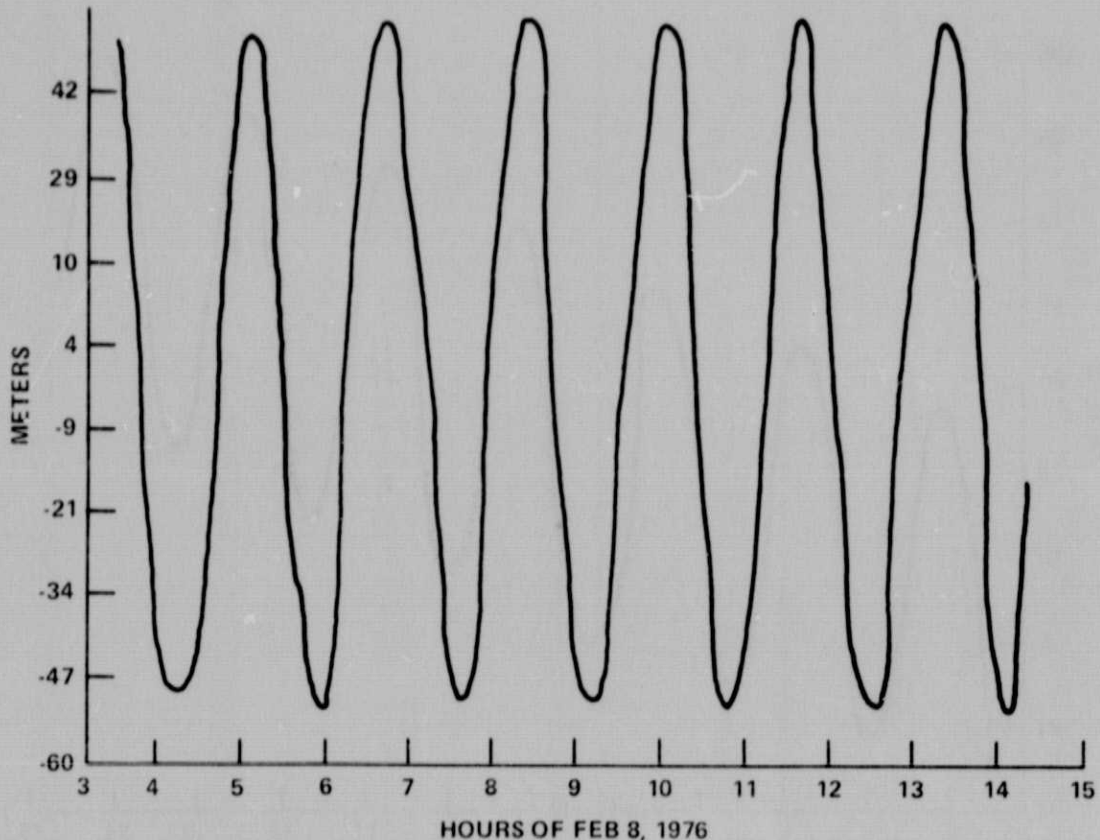

Figure 11. Cross Track Differences for Nimbus-6 Satellite-to-Satellite Tracking Orbit Determination

factor in an orbit determination with satellite-to-satellite radio tracking appears to be the accuracy of the force models rather than tracking system precision.

The results of these experiments imply that with the proper data reduction procedures, the tracking data relay satellite system should provide orbit determination capability comparable to what is now obtainable from ground based systems.

ACKNOWLEDGMENTS

The authors thank Dr. Georg Morduch and Mr. John Bryan for their aid during the course of this research.

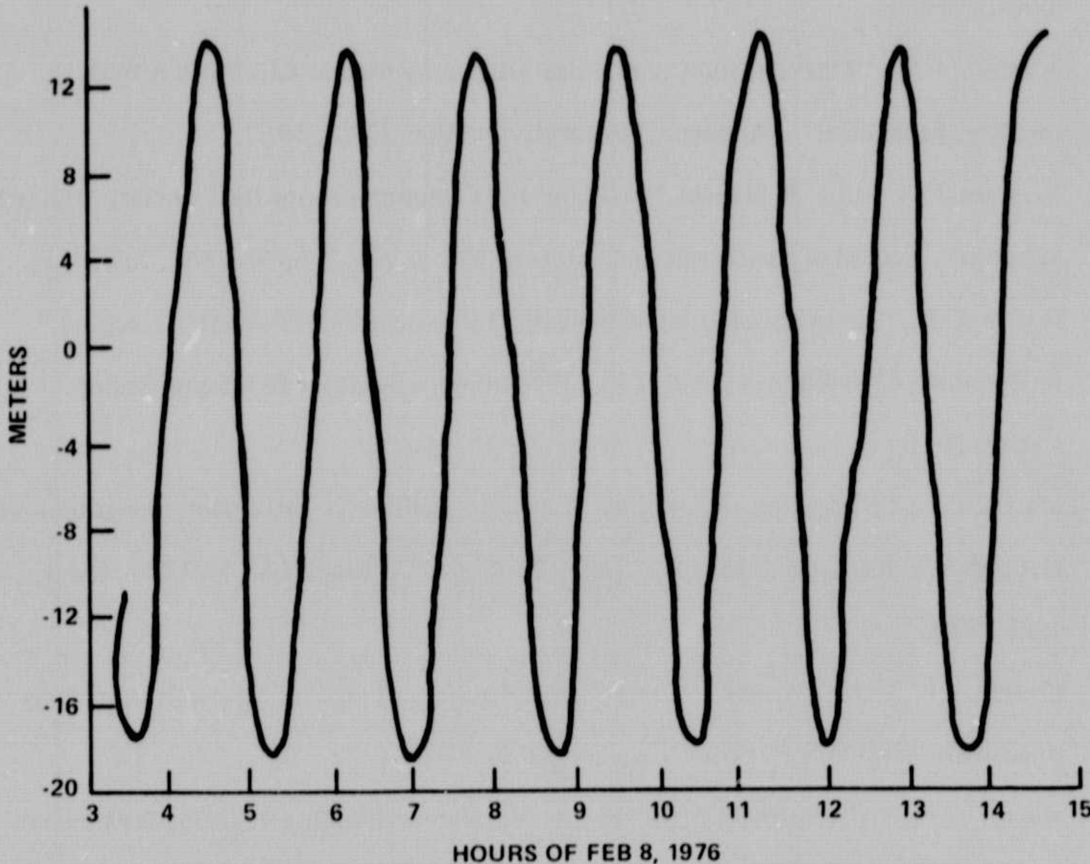

Figure 12. Radial Differences for Nimbus-6 Satellite-to-Satellite Tracking Orbit Determination

ORIGINAL PAGE IS
OF POOR QUALITY

REFERENCES

1. Bergaust, E. and W. Beller, "Satellite", p. 135, Hanover House, Garden City, New York, 1956.

2. Vonbun, F.O., "Tracking and Communications" presented at AIAA 4th Annual meeting, paper 67-976, Anaheim, California, October 23-27, 1967.

3. Vonbun, F.O. and J. T. Mengel, "Tracking and Communications for Planetary Manned Missions", Journal of Spacecraft and Rockets, Vol. 5, No. 7, pp 863-865, July 1968.

4. Martin, C.F., "Accuracy of Orbits Obtainable by Synchronous Satellites Tracking," in Dynamics of Satellites (1969), 120-129, edited by B. Morando (Berlin, Spring Verlag, 1970.

5. Martin, C.F., "Evaluation of Satellites Tracking Satellites for Orbit Determination and Geopotential Recovery," Final Technical Report on Contract NAS 5-11736-Mod 3, June 1970.

6. Cooley, J.L., and A. Marlow, "Orbital Error Studies – Tracking from a Synchronous Spacecraft," GSFC X-551-69-7, January 1969.

7. Martin, C.F., T.V. Martin and D.E. Smith, "Satellite-to-Satellite Tracking for Estimating Geopotential Coefficients," The Use of Artificial Satellites for Geodesy, AGU Mono. 15, 139-144, 1972.

8. Schwarz, C.R., "Refinement of the Gravity Field by Satellite-to-Satellite Doppler Tracking," The Use of Artificial Satellites for Geodesy, AGU Mono. 15, 133-138, 1972.

9. Kaula, W.M., "Error Analysis of Earth Physics Satellite Systems," Final Report, Part I, on NASA Grant No. NGR 05-007-280, October 1972.

10. Heffernan, P.J., "ATS-F/NIMBUS-F Tracking and Data Relay Experiment Technical Summary", NASA-GSFC, 3 October 1968.

11. Vonbun, F.O., et al., "Gravity Anomaly Detection – Apollo/Soyuz", NASA-GSFC X-920-75-308, December, 1975.

12. Teles, J., Ayres, C., "Advanced Spacecraft Tracking Techniques Using the Tracking and Data Relay Satellite System", presented at the AAS/AIM Astrodynamics Conference, Sept. 7-9, 1977, Grand Teton National Park, Wyoming.

13. Schmid, P.E. and F.O. Vonbun, "The ATS-F/NIMBUS-F Tracking and Orbit Determination Experiment", 1974 IEEE INTERCON, New York City.

14. Schmid, P.E., F.O. Vonbun, and B.J. Trudell, "ATS-6 Satellite-to-Satellite Tracking and Data Relay Experiments", pp. 1048-1058, IEEE Transactions on Aerospace and Electronic Systems, Vol. AES-11, No. 6, November 1975.

15. Vonbun, F.O., "Geodetic Satellite Missions and GEOS-C Spacecraft", Space Research XI-Akademic-Verlag, Berlin 1971.

16. Vonbun, F.O. et al., Geodynamics Experiment MA-128, Apollo-Soyuz test Project, Preliminary Science Report, NASA TMX-58173, February 1976.

17. Vonbun, F.O., "The ATS-F/NIMBUS-E Tracking Experiment", pp. 112-120, "Rotation of the Earth", P. Mechior & S. Yumi (eds), D. Reidel Publishing Co., Dordrecht, Holland, 1972.

18. Schmid, P.E., "The Tracking and Data Relay Experiment (T&DRE)", pp. 207-218, The NIMBUS-6 User's Guide NASA-GSFC, February 1975.

19. Marini, J.W., "Doppler Factors in Satellite-to-Satellite Tracking", NASA-GSFC X-932-74-93, April 1974.

20. Schmid, P.E., R.B. Bent, S.K. Llewellyn, G. Nesterczuk, and S. Rangaswamy, NASA-"GSFC Ionospheric Corrections to Satellite Tracking Data", NASA-GSFC X-591-73-281, December 1973.

21. Marini, J.W., "Correction of Satellite Tracking Data for an Arbitrary Tropospheric Profile", Radio-Science Volume 7, No. 2, pages 223-231, February 1972.

22. Marini, J.W., "Tropospheric Range-Rate Tracking Data Correction", NASA-GSFC X-551-72-277, August 1972.

23. Argentiero, P., and Loveless, F., "Orbit Determination with the Tracking Data Relay Satellite System", NASA-GSFC X-932-76-185, February 1977.

24. Clark, George Q., "Tracking and Data Relay Satellite Systems (TDRSS) User's Guide", STDN, No. 101.2, NASA-GSFC Greenbelt, Maryland, May 1975.

25. Fang, B., and Gibbs, B., "TDRSS Era Orbit Determination System Review Study", Planetary Sciences Department Report No. MT010-75, Wolf Research and Development Group, December 1975.

26. Argentiero, P., and Garza-Robles, R., "GEOS-C Orbit Determination With Satellite-to-Satellite Tracking", Journal of the Astronautical Sciences, Vol. XXIII, No. 3, pp 241-256, July - September 1975.

27. Schmid, P.E., Argentiero, P., and Vonbun, F.O., "Satellite-to-Satellite System and Orbital Error Estimates", presented at the Precision Time and Time Interval Conference, NASA-GSFC, December 2-4, 1975.

28. Schmid, P.E. and J.J. Lynn, "Results of the 3 November 1974 Applications Technology Satellite-6 (ATS-6) Trilateration Test", NASA/GSFC X-932-75-104, April 1975.

29. Lynn, J.J., P.E. Schmid and R.E. Anderson, "A New Method for Satellite Orbit Determination Using an Operational Worldwide Transponder Network", NASA-GSFC X-591-74-2, January 1974.

30. Vonbun, F.O., "Satellite Trajectory Determination and Their Expected Errors OGO-IV, GEOS-1" Dynamics of Satellites (1969), p. 89-103, Springer-Verlog, Berlin, Heidelberg, New York, 1970.

31. Marsh, J., Goddard Space Flight Center, Private Communications.